Acta Crystallographica Section D
Biological Crystallography
ISSN 0907-4449

The production and purification of the human T-cell receptors, the CD3$\varepsilon\gamma$ and CD3$\varepsilon\delta$ heterodimers: complex formation and crystallization with OKT3, a therapeutic monoclonal antibody

Michelle A. Dunstone,[a]‡ Lars Kjer-Nielsen,[b]‡ Lyudmila Kostenko,[b] Anthony W. Purcell,[b] Andrew G. Brooks,[b] Jamie Rossjohn[a]* and James McCluskey[b]

[a]The Protein Crystallography Unit, Department of Biochemistry and Molecular Biology, School of Biochemical Sciences, Monash University, Clayton, Victoria 3800, Australia, and [b]Department of Microbiology and Immunology, University of Melbourne, Parkville, Victoria 3010, Australia

‡ These authors contributed equally.

Correspondence e-mail: jamie.rossjohn@med.monash.edu.au, jamesm1@unimelb.edu.au

Received 1 March 2004
Accepted 18 May 2004

Human CD3 is an essential multisubunit complex that plays a fundamental role in T-cell signalling, T-cell development and surface expression of the $\alpha\beta$ T-cell receptor. The CD3 complex comprises the CD3$\varepsilon\gamma$ and CD3$\varepsilon\delta$ heterodimers and the CD3$\zeta\zeta$ homodimer. Here, the expression of the human CD3$\varepsilon\gamma$ and CD3$\varepsilon\delta$ heterodimers, both of which were expressed as single-chain polypeptides, is reported. Following refolding, functional heterodimers were immunoaffinity purified from improperly folded heterodimers using OKT3, a therapeutic monoclonal antibody specific for the CD3ε chain. Subsequently, the Fab fragment of OKT3 was used to complex individually with the CD3$\varepsilon\gamma$ and CD3$\varepsilon\delta$ heterodimers. Crystals of scCD3$\varepsilon\gamma$–FabOKT3 were grown using 15%(*w*/*v*) PEG 3350, 200 m*M* potassium fluoride, 100 m*M* Tris–HCl pH 8.0. Crystals of scCD3$\varepsilon\delta$–FabOKT3 were grown using 20%(*w*/*v*) PEG 3350, 200 m*M* potassium formate, 100 m*M* Tris–HCl pH 8.0, 2%(*v*/*v*) MPD. Crystals of both complexes diffract to beyond 3 Å resolution. scCD3$\varepsilon\gamma$–FabOKT3 crystals belonged to space group $P2_1$, with unit-cell parameters a = 67.70, b = 55.77, c = 96.05 Å, β = 100.85° and one complex per asymmetric unit. scCD3$\varepsilon\delta$–FabOKT3 crystals belong to space group $P2_1$, with unit-cell parameters a = 101.67, b = 50.36, c = 138.7 Å, β = 108.84°, suggesting two complexes per asymmetric unit.

1. Introduction

Cytotoxic T cells (CTLs) are responsible for scanning host cells for signs of viral infection or aberrant cell growth, as observed in tumour cells. This recognition process is mediated by the clonotypically distributed $\alpha\beta$ T-cell receptor (TCR) that interacts with peptide-laden molecules of the major histocompatibility complex (MHC; Davis & Bjorkman, 1988). This specific recognition event signals the CTL to eliminate the target cell. The $\alpha\beta$ TCR does not possess signalling domains; instead, the initial CTL signalling function resides within the conserved multisubunit signalling apparatus CD3. The ε, γ, δ and ζ subunits of the CD3 signalling complex associate with each other to form a CD3$\varepsilon\gamma$ heterodimer, a CD3$\varepsilon\delta$ heterodimer and a CD3$\zeta\zeta$ homodimer (Call *et al.*, 2002; Alarcon *et al.*, 2003). *In vitro* and *in vivo* studies have revealed that the CD3 subunits not only play a critical role in T-cell signalling, but are also required for the cell-surface expression of the $\alpha\beta$ TCR and normal T-cell development (Alarcon *et al.*, 2003).

The CD3γ, δ and ε subunits consist of one extracellular immunoglobin (Ig) domain, a conserved cysteine-rich stalk, a transmembrane domain and a cytoplasmic domain that contains the intracellular immunoreceptor tyrosine-activation motifs (ITAM; Malissen, 2003). Recently, the solution structure of the ectodomain fragments of the mouse CD3$\varepsilon\gamma$ heterodimer showed that the CD3ε and γ subunits interact with each other to form an unusual side-to-side dimer configuration (Sun *et al.*, 2001). The CD3 subunits not only interact with each other, but also interact with the $\alpha\beta$ TCR *via* charged residues located in the transmembrane α-helices, as well as association *via* the respective ectodomains. For example, one candidate site for interaction is *via* the FG loop of the constant domain of the TCR β chain (Wang *et al.*, 1998). However, sequence differences between CD3 subunits across species suggest variations in their mode of interaction within the TCR complex (LeFranc, 2001).

Anti-human CD3 monoclonal antibodies are widely used clinically in immunosuppressive regimes (Chatenoud, 2003). For example, OKT3, the prototypical anti-CD3 monoclonal antibody, has been used in anti-rejection therapy in transplantation since gaining FDA approval in 1985. Moreover, a humanized version of OKT3 has also been used as a tolerogenic agent in the treatment of autoimmune diseases such as type 1 diabetes (Masteller & Bluestone, 2002) and psoriasis (Utset *et al.*, 2002). Although there are multiple modes of action regarding OKT3

administration, its activity depends upon the specific interaction with the CD3ε component (Chatenoud, 2003).

In order to gain greater insights into the architecture of human CD3$\varepsilon\gamma$ and CD3$\varepsilon\delta$ and to compare them with their murine counterparts, the ectodomains of the CD3 subunits were expressed in *Escherichia coli* as a single-chain construct with a 26-amino-acid linker connecting the two subunits. To aid in the purification of the correctly refolded CD3 heterodimers, an OKT3 immunoaffinity chromatography step was used. In addition, to begin to gain a greater understanding of the mode of OKT3 binding to CD3ε, Fab fragments of OKT3 were subsequently generated and used to form complexes with CD3$\varepsilon\delta$ and CD3$\varepsilon\gamma$. These complexes were stable enough to undergo further purification by gel filtration as well as crystallization studies. Crystals of the scCD3$\varepsilon\gamma$–FabOKT3 and scCD3$\varepsilon\delta$–FabOKT3 complexes were obtained and preliminary diffraction analysis is under way.

2. Methods

2.1. Cloning of CD3 ectodomains

CD3ε, CD3γ and CD3δ were cloned from the human Epstein–Barr virus-specific HLA-B8-restricted T-cell clone CF34 (Burrows *et al.*, 1994). RNA was reverse-transcribed with reverse transcriptase using oligo-dT to prime. cDNA was PCR-amplified using complementary oligonucleotides to the region encoding the single extracellular immunoglobulin-like domain, terminating immediately prior to the amino-terminus of the C*XX*C*X*E motif in the stalk region (Sun *et al.*, 2001). The region of cDNA amplified is as follows: CD3ε (accession code P07766, residues 23–118), CD3γ (accession code P09693, residues 23–103) and CD3δ (accession code P04234, residues 22–92). These PCR-amplified DNA fragments were T-A-cloned into the plasmid vector P-GEM T Easy (Promega) and the cloned gene segments were verified by sequencing. Two single-chain constructs were made, in which a 26-residue linker peptide (GSADDAKKDA AKKDDAKK-DD AKKDGS) connected the C-terminus of CD3γ to the N-terminus of CD3ε (scCD3$\varepsilon\gamma$) and the C-terminus of CD3δ to the N-terminus of CD3ε (scCD3$\varepsilon\delta$) (Fig. 1). To make the chimeric CD3 genes, each CD3 gene was PCR-amplified with an oligonucleotide encoding part of the linker peptide. For the CD3ε gene this was located at the 5′ end and for the CD3γ and CD3δ genes this was located at the 3′ end of the amplimer. The PCR amplimers thus obtained had 31 base-pair complementarity and were then used as templates for a PCR reaction creating the chimeric genes. Both PCR products were cloned as an *Nde*I–*Hin*dIII fragment into the pET-30 expression vector (Novagen).

2.2. Expression and purification of the scCD3$\varepsilon\gamma$ and scCD3$\varepsilon\delta$ heterodimers

Inclusion-body preparations expressed by *E. coli* of the scCD3$\varepsilon\gamma$ and scCD3$\varepsilon\delta$ proteins were prepared essentially as per the method of Garboczi *et al.* (1996). 45 mg of scCD3$\varepsilon\gamma$ and scCD3$\varepsilon\delta$ inclusion-body preparation was thawed and injected into 400 ml of stirring refolding buffer containing 200 m*M* Tris–HCl pH 8.5, 0.8 *M* arginine, 1 m*M* oxidized glutathione, 0.2 m*M* reduced glutathione, 0.2 m*M* PMSF, 1 µg ml^{-1} pepstatin A at 277 K for 24 h. The refolded protein was dialysed (Spectrum; molecular-weight cutoff 6000–8000 kDa) against three changes of 10 l phosphate-buffered saline (PBS) for 4, 4 and 16 h, respectively.

2.3. Production of OKT3 and immunoprecipitation experimentation

Supernatant containing OKT3 was harvested from cells grown in Xten Hybricell serum-free medium (ThermoTrace) in miniPerm production modules (Vivascience). OKT3 was purified from supernatant using a Protein A Sepharose 4 Fast Flow column (Amersham Pharmacia) and eluted according to the manufacturers' instructions. For long-term storage, purified OKT3 was dialyzed against PBS and concentrated sodium azide was added to a final concentration of 0.02%(*w*/*v*). Immunoprecipitation experiments utilized OKT3 to analyse the conformation of the refolded scCD3$\varepsilon\gamma$ heterodimer. Immunoprecipitation was performed according to Kim *et al.* (2000) and the results were analysed by non-reducing SDS–PAGE. 50 mg OKT3 was immobilized as according to Kim *et al.* (2000), forming an immunoaffinity column.

2.4. Purification of scCD3$\varepsilon\gamma$ and scCD3$\varepsilon\delta$ heterodimers

Dialysed scCD3$\varepsilon\gamma$ or scCD3$\varepsilon\delta$ heterodimer was captured on an OKT3 immunoaffinity column containing 50 mg immobilized OKT3. The column was washed with PBS and the bound scCD3 heterodimer was eluted with 50 m*M* citrate pH 3.0, 20 m*M* Tris–HCl and 0.1 *M* NaCl. Peak fractions were immediately adjusted to pH 7.2–7.5 using 1 *M* Tris–HCl pH 8.5. Fractions containing the eluted scCD3 heterodimer were pooled, buffer-exchanged into 10 m*M* Tris–HCl, 150 m*M* NaCl pH 8.0 and concentrated to 2 ml in preparation for gel filtration. The concentrated protein solution was loaded onto a HiLoad 16/60 Superdex 75 pg gel-filtration column (Amersham Pharmacia, Uppsala, Sweden) in the presence of 10 m*M* Tris–HCl, 150 m*M* NaCl pH 8.0. Fractions containing scCD3 heterodimer were pooled. The final purified protein solution was concentrated to 5–10 mg ml^{-1} and analysed by non-reducing SDS–PAGE.

2.5. Generation of OKT3 Fab fragments

Fab fragments of OKT3 (FabOKT3) were produced using the ImmunoPure Fab Preparation Kit (Pierce). To purify the Fab fragments from the Fc fragments, the digest was passed over a Protein A Sepharose 4 Fast Flow column and the flowthrough containing FabOKT3 was concentrated and buffer-exchanged to 10 m*M* Tris–HCl pH 8.0. FabOKT3 was then further purified by anion-exchange chromatography on a Mono Q HR 10/10 column (Amersham Pharmacia) in buffer containing 10 m*M* Tris pH 8.0 over a gradient of 0–1 *M* NaCl. FabOKT3 eluted at approximately 340 m*M* NaCl. The final gel-filtration purification step utilized a HiLoad 16/60 Superdex 75 column (Amersham Pharmacia).

2.6. Purification of scCD3 heterodimer–FabOKT3 complex

To generate scCD3$\varepsilon\gamma$ and scCD3$\varepsilon\delta$ complexed with FabOKT3, a 2.6-fold molar

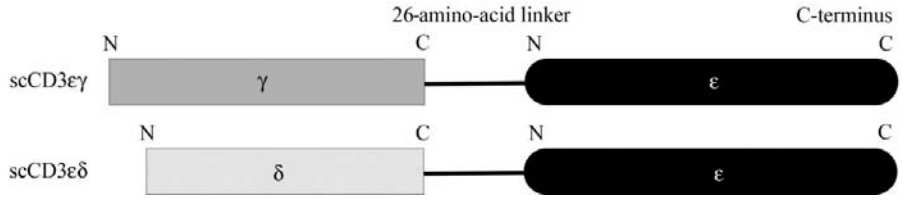

Figure 1
Schematic of the domain arrangements used to express the CD3$\varepsilon\gamma$ and CD3$\varepsilon\delta$ heterodimers as single chains. N and C denote the N-terminal and C-terminal regions, respectively. The box sizes are proportional to the relative sequence length of the open reading frames for each of the CD3 domains.

excess of purified scCD3$\varepsilon\gamma$ or scCD3$\varepsilon\delta$ was incubated for 16 h with FabOKT3 in 10 m*M* Tris–HCl and 150 m*M* NaCl pH 8.0 at 277 K. This mixture was then passed over a 16/60 Superdex 75 column and CD3 heterodimer complexed with FabOKT3 was resolved from excess free CD3 heterodimer. The scCD3 heterodimers complexed with FabOKT3, named scCD3$\varepsilon\gamma$–FabOKT3 and scCD3$\varepsilon\delta$–FabOKT3, were concentrated and used for crystallization trials.

2.7. Crystallization and data collection

Crystallization experiments were performed at room temperature using the hanging-drop vapour-diffusion technique. Solutions of purified scCD3$\varepsilon\gamma$–FabOKT3 and scCD3$\varepsilon\delta$–FabOKT3 were concentrated to 5–8 mg ml^{-1} (in the buffer 10 m*M* Tris–HCl, 200 m*M* NaCl pH 8.0) and screened in the commercially available PEG/Ion Screen and Crystal Screen (Hampton Research, Laguna Niguel, USA).

In order to analyse the crystal composition, large crystals were washed three times in 5 µl equilibrated mother liquor and then dissolved in 20 µl MilliQ water. Small crystals were analysed by harvesting the entire drop and resuspending by gentle pipetting in 20 µl mother liquor. This mixture was centrifuged at 5000*g* for 5 min at room temperature. 17 µl supernatant was carefully removed by pipette and discarded, while the final ∼3 µl was kept. This wash procedure was performed a further two times. The remaining 3 µl, which contained the washed crystals, was resuspended by vortexing in 20 µl MilliQ water and incubating at 310 K with intermittent shaking for 4 h. Samples of dissolved crystals were analysed by silver-stained non-reducing SDS–PAGE.

The optimized condition for growing crystals of scCD3$\varepsilon\gamma$–FabOKT3 crystals involved mixing equal volumes of 5 mg ml^{-1} scCD3$\varepsilon\gamma$–FabOKT3 solution with reservoir buffer: 15%(*w*/*v*) PEG 3350, 200 m*M* potassium fluoride, 100 m*M* Tris–HCl pH 8.0. The crystals were flash-frozen prior to data collection using 20%(*w*/*v*) glycerol as the cryoprotectant.

Diffraction-quality crystals of scCD3$\varepsilon\delta$–FabOKT3 were grown by mixing equal volumes of 8 mg ml^{-1} scCD3$\varepsilon\delta$–FabOKT3 with a reservoir buffer consisting of 20%(*w*/*v*) PEG 3350, 200 m*M* potassium formate, 100 m*M* Tris–HCl pH 8.0, 2%(*v*/*v*) MPD. These crystals were flash-frozen directly into liquid nitrogen prior to diffraction analysis. 15%(*w*/*v*) glycerol was used as the cryoprotectant in a solution consisting of 22%(*w*/*v*) PEG 3350, 200 m*M* potassium formate, 100 m*M* Tris pH 8.0, 2%(*v*/*v*) MPD.

All data were collected in-house on an R-AXIS IV^{++} detector with Cu $K\alpha$ X-rays generated by a Rigaku RU-H3RHB rotating-anode generator and focused using Osmic mirrors. Data were collected from the frozen crystals using inverse-φ geometry. The scCD3$\varepsilon\gamma$–FabOKT3 data set comprised 438 images (0.3° oscillation, 20 min exposure per oscillation). Several scCD3$\varepsilon\delta$–FabOKT3 crystals were indexed from single images. The diffraction data were processed and analysed using the *HKL* package (Table 1) (Otwinowski & Minor, 1997).

3. Results and discussion

3.1. Purification of the scCD3 heterodimers

After refolding of scCD3$\varepsilon\gamma$, a doublet band was observed on non-reducing SDS–PAGE (Fig. 2, lane 1), whereas reducing SDS–PAGE showed scCD3$\varepsilon\gamma$ to migrate as a single species (data not shown), suggesting that either one or both scCD3$\varepsilon\gamma$ bands contained an incorrect disulfide-bonding pattern. The refolded scCD3$\varepsilon\gamma$ preparation was analysed by OKT3 immunoprecipitation in order to determine whether an OKT3-dependent conformational difference existed between the two species. The upper species of the doublet bands alone bound to OKT3, while the lower species did not, suggesting that the upper scCD3$\varepsilon\gamma$ band represented a correctly folded heterodimer (Fig. 2, lane 2). The two species were unable to be separated by ion-exchange chromatography or hydrophobic interaction chromatography (data not shown). Changing the scCD3$\varepsilon\gamma$ construct so that the C-terminus of CD3ε was linked to the N-terminus of CD3γ (similar to the construct reported for murine scCD3$\varepsilon\gamma$; Kim *et al.*, 2000) resulted in a greater proportion of the scCD3$\varepsilon\gamma$ being aberrantly refolded (data not shown). To separate the two species, the correctly refolded scCD3$\varepsilon\gamma$ was purified using an OKT3-immunoaffinity step followed by gel filtration. This protocol resulted in a homogeneous scCD3$\varepsilon\gamma$ species that was confirmed by mass spectrometry to be of the correct molecular weight. Similarly, scCD3$\varepsilon\delta$ was expressed and purified to homogeneity using the protocol established for scCD3$\varepsilon\gamma$ (data not shown).

Both complexes of FabOKT3 with scCD3$\varepsilon\gamma$ or scCD3$\varepsilon\delta$ were successfully formed and purified by gel filtration from the excess uncomplexed scCD3 heterodimer. scCD3$\varepsilon\gamma$–FabOKT3 elutes separately from the excess scCD3$\varepsilon\gamma$ and at the correct molecular weight of approximately 73 kDa, while purification of scCD3$\varepsilon\delta$–FabOKT3 gave a similar elution profile (data not shown).

Table 1
Data-collection statistics for the scCD3$\varepsilon\gamma$–OKT3 complex.

Values in parentheses are for the highest resolution bin (approximately 0.1 Å).

Temperature (K)	100
Space group	$P2_1$
Unit-cell parameters	
a (Å)	67.70
b (Å)	55.77
c (Å)	96.05
β (°)	100.85
Resolution range (Å)	20–2.1
Total No. observations	111297 (10866)
No. unique observations	41156 (4110)
Multiplicity	2.7 (2.6)
Data completeness (%)	99.4 (100)
$I/\sigma(I) > 2$ (%)	80.5 (61.4)
$\langle I/\sigma(I)\rangle$	12.9 (3.4)
$R_{\rm merge}$† (%)	9.3 (43.8)

† $R_{\rm merge} = \sum |I_{hkl} - \langle I_{hkl}\rangle| / \sum I_{hkl}$.

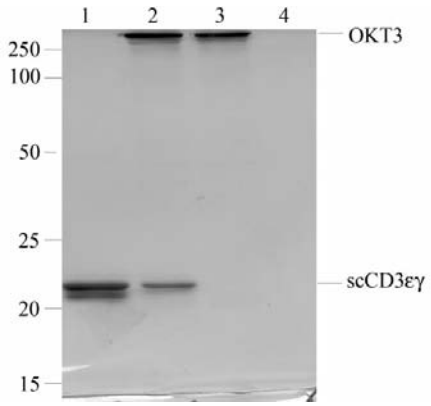

Figure 2
Non-reducing SDS–PAGE of the immunoprecipitation results. Lane 1, scCD3$\varepsilon\gamma$ before immunoprecipitation; lane 2, immunoprecipitation of the upper band of scCD3$\varepsilon\gamma$ with OKT3; lane 3, OKT3 only; lane 4, scCD3$\varepsilon\gamma$ only.

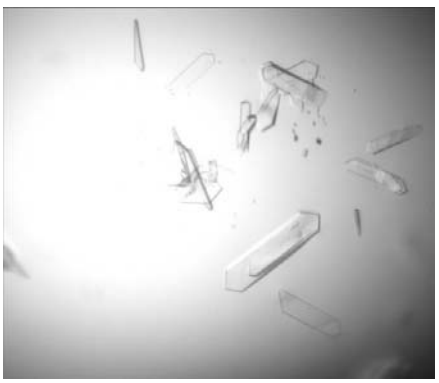

Figure 3
Diffraction-quality crystals of the scCD3$\varepsilon\gamma$–FabOKT3 complex.

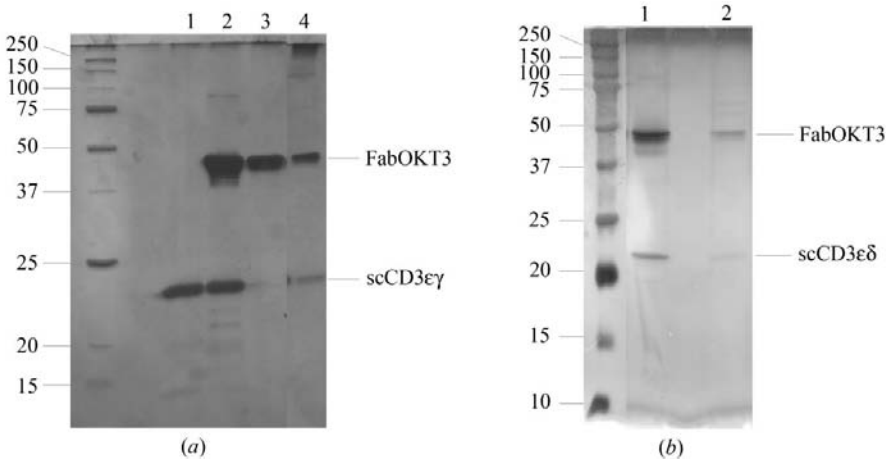

Figure 4
Silver-stained non-reducing SDS–PAGE was used to analyse crystal composition. (*a*) Analysis of a dissolved scCD3$\varepsilon\gamma$–FabOKT3 crystal. Lane 1, scCD3$\varepsilon\gamma$ only; lane 2, scCD3$\varepsilon\gamma$–FabOKT3 stock material; lane 3, FabOKT3 only; lane 4, washed and dissolved crystals of scCD3$\varepsilon\gamma$–FabOKT3. (*b*) Analysis of a dissolved scCD3$\varepsilon\delta$–FabOKT3 crystal. Lane 1, scCD3$\varepsilon\delta$–FabOKT3 stock material; lane 2, washed and dissolved crystals of scCD3$\varepsilon\delta$–FabOKT3.

3.2. Crystallization of scCD3$\varepsilon\gamma$–FabOKT3 and scCD3$\varepsilon\delta$–FabOKT3

Crystals grew under many different conditions, particularly in the PEG/Ion Screen; however, many of these crystals were shown to consist of only FabOKT3 by silver-stained non-reducing SDS–PAGE analysis (data not shown). A number of candidate crystal conditions for the complex scCD3$\varepsilon\gamma$–FabOKT3 were identified and, of these conditions, one was identified in which improved plate-like crystals of the scCD3$\varepsilon\gamma$–FabOKT3 complex grew (Figs. 3 and 4*a*). Crystals of scCD3$\varepsilon\gamma$–FabOKT3 from the optimized condition diffracted to 2.1 Å and a complete native data set was collected (Table 1). A Matthews coefficient of 2.4 Å^3 Da^{-1} corresponds to a solvent content of 50%, consistent with one scCD3$\varepsilon\gamma$–FabOKT3 complex per asymmetric unit.

As with the scCD3$\varepsilon\gamma$–FabOKT3 complex, crystal screens of the scCD3$\varepsilon\delta$–FabOKT3 complex resulted in a number of FabOKT3-only crystals. Many crystals which diffracted were consistently confirmed to consist of the scCD3$\varepsilon\delta$–FabOKT3 complex by silver-stained SDS–PAGE (Fig. 4*b*). These crystals belong to space group $P2_1$, with unit-cell parameters $a = 101.67$, $b = 50.36$, $c = 138.7$ Å, $\beta = 108.84^\circ$. Crystals grown from the optimal conditions diffracted to 3.0 Å resolution. A Matthews coefficient of 2.4 Å^3 Da^{-1} corresponds to a solvent content of approximately 48%, consistent with two scCD3$\varepsilon\delta$–FabOKT3 complexes per asymmetric unit.

Given that antibody–antigen interactions are generally of high affinity, it was moderately surprising to find that the complex readily dissociated during the crystallization trials, suggesting the affinity for this particular interaction is relatively weak. The three-dimensional structure of scCD3$\varepsilon\gamma$–FabOKT3 has been successfully determined and is published elsewhere (Kjer-Nielsen *et al.*, 2004). Coordinates have been deposited in the PDB (code 1sy6). This work will provide us with detailed insights into the mode of CD3 dimerization, provide an invaluable comparison to the murine counterpart CD3$\varepsilon\gamma$ (Sun *et al.*, 2001) and allow us to address the mode of OKT3 binding.

JR is supported by a Wellcome Trust Senior Research Fellowship in Biomedical Science in Australia; AP is supported by a Melbourne University CR Roper Fellowship. This work was supported by the NH&MRC Australia and the Australian Research Council.

References

Alarcon, B., Gil, D., Delgado, P. & Schamel, W. W. (2003). *Immunol. Rev.* **191**, 38–46.
Burrows, S. R., Khanna, R., Burrows, J. M. & Moss, D. J. (1994). *J. Exp. Med.* **179**, 1155–1161.
Call, M. E., Pyrdol, J., Wiedmann, M. & Wucherpfennig, K. W. (2002). *Cell*, **111**, 967–979.
Chatenoud, L. (2003). *Nature Rev. Immunol.* **3**, 123–132.
Davis, M. M. & Bjorkman, P. J. (1988). *Nature (London)*, **334**, 395–402.
Garboczi, D. N., Utz, U., Ghosh, P., Seth, A., Kim, J., VanTienhoven, E. A., Biddison, W. E. & Wiley, D. C. (1996). *J. Immunol.* **157**, 5403–10.
Kim, K. S., Sun, Z. Y., Wagner, G. & Reinherz, E. L. (2000). *J. Mol. Biol.* **302**, 899–916.
Kjer-Nielsen, L., Dunstone, M. A., Kostenko, L., Ely, L. K., Beddoe, T., Misfud, N. A., Purcell, A. W., Brooks, A. G., McCluskey, J. & Rossjohn, J. (2004). *Proc. Natl Acad. Sci. USA*, **101**, 7675–7680.
Lefranc, M. P. (2001). *Nucleic Acids. Res.* **29**, 207–209.
Malissen, B. (2003). *Immunol. Rev.* **191**, 7–27.
Masteller, E. L. & Bluestone, J. A. (2002). *Curr. Opin. Immunol.* **14**, 652–659.
Otwinowski, Z. & Minor, W. (1997). *Methods Enzymol.* **276**, 307–326.
Sun, Z. J., Kim, K. S., Wagner, G. & Reinherz, E. L. (2001). *Cell*, **105**, 913–923.
Utset, T. O., Auger, J. A., Peace, D., Zivin, R. A., Xu, D., Jolliffe, L., Alegre, M. L., Bluestone, J. A. & Clark, M. R. (2002). *J. Rheumatol.* **29**, 1907–1913.
Wang, J., Lim, K., Smolyar, A., Teng, M., Liu, J., Tse, A. G., Liu., J., Hussey, R. E., Chistri, Y., Thomson, C. T., Sweet, R. M., Nathenson, S. G., Chang, H. C., Sacchettini, J. C. & Reinherz, E. L. (1998). *EMBO J.* **17**, 10–26.